FEBS Letters 582 (2008) 1032–1036

Crystal structure of the *Clostridium limosum* C3 exoenzyme

Martin Vogelsgesang[a,1], Benjamin Stieglitz[b,2], Christian Herrmann[b], Alex Pautsch[c], Klaus Aktories[a,*]

[a] *Institut für Experimentelle und Klinische Pharmakologie und Toxikologie der Albert-Ludwigs-Universität Freiburg, Otto-Krayer-Haus, Albertstrasse 25, D-79104 Freiburg, Germany*
[b] *Physikalische Chemie I, Ruhr-Universität Bochum, Universitätsstraße 150, D-44780 Bochum, Germany*
[c] *Department of Lead Discovery, Boehringer Ingelheim Pharma GmbH & Co. KG, D-88397 Biberach an der Riss, Germany*

Received 3 January 2008; revised 25 February 2008; accepted 25 February 2008

Available online 4 March 2008

Edited by Hans Eklund

Abstract C3-like toxins ADP-ribosylate and inactivate Rho GTPases. Seven C3-like ADP-ribosyltransferases produced by *Clostridium botulinum*, *Clostridium limosum*, *Bacillus cereus* and *Staphylococcus aureus* were identified and two representatives – C3bot from *C. botulinum* and C3stau2 from *S. aureus* – were crystallized. Here we present the 1.8 Å structure of *C. limosum* C3 transferase C3lim and compare it to the structures of other family members. In contrast to the structure of apo-C3bot, the canonical ADP-ribosylating turn turn motif is observed in a primed conformation, ready for NAD binding. This suggests an impact on the binding mode of NAD and on the transferase reaction. The crystal structure explains why auto-ADP-ribosylation of C3lim at Arg41 interferes with the ADP-ribosyltransferase activity of the toxin.

Keywords: ADP-ribosyltransferase; Exoenzyme C3; Rho GTPase; Crystal structure; Toxin

1. Introduction

Various bacterial toxins and effectors interfere with eukaryotic cell functions by ADP-ribosylation of essential cellular proteins [1–4]. A typical example is the family of C3-like ADP-ribosyltransferases [5,6]. It comprises the prototype *Clostridium botulinum* exoenzyme C3bot [7], including the isoforms C3bot1 and C3bot2, the exoenzyme from *Clostridium limosum* (C3lim) [8], *Bacillus cereus* C3 transferase (C3cer) [9] and three isoforms of C3stau from *Staphylococcus aureus* also called EDIN [10,11].

*Corresponding author. Fax: +49 761 2035311.
E-mail address: Klaus.Aktories@pharmakol.uni-freiburg.de (K. Aktories).

[1]Present address: Novartis Pharma AG, Lichtstrasse 35, CH-4056 Basel, Switzerland.
[2]Presented address: Medical Research Council National Institute for Medical Research, Division of Molecular Structure, The Ridgeway, Mill Hill, London NW7 1AA, United Kingdom.

Abbreviations: ARTT-motif, ADP-ribosylation toxin turn turn motif; C3bot, C3 ADP-ribosyltransferase from *Clostridium botulinum*; C3cer, C3 ADP-ribosyltransferase from *Bacillus cereus*; C3lim, C3 ADP-ribosyltransferase from *Clostridium limosum*; C3stau2, C3 ADP-ribosyltransferase from *Staphylococcus aureus*; GST, glutathione *S*-transferase

Hallmark of these exoenzymes is the selective *N*-ADP-ribosylation of the low-molecular mass GTP-binding proteins RhoA, B and C onto the acceptor amino acid Asn41 [12–14], resulting in the biological inactivation of signal pathways controlled by Rho GTPases [15]. Consequently, C3-like exoenzymes have been valuable pharmacological tools for the analysis of cellular functions of Rho proteins [5,6]. Whereas these exoenzymes harbor the enzyme activity, they apparently miss any specific cell binding and transportation unit and therefore, differ from typical AB-toxins, which contain in addition to the enzyme domain a unit for cell binding and transportation [5].

C3 transferases are basic 23–25 kDa proteins, which are 30–77% identical to each other in their amino acid sequences. Although C3-like ADP-ribosyltransferases share only limited sequence similarity, key amino acid residues and short peptide stretches are conserved in all of them. Recently, the crystal structures of C3bot1 and C3stau2 either unbound or bound to NAD were reported [16–18], while structures of other family members have been lacking so far. Together with data derived from biochemical studies and site-directed mutagenesis [19–21], the available structure analyses largely improved our understanding of the mechanism of the ADP-ribosylation reaction of Rho-ADP-ribosylating transferases. Accordingly, the active site is delineated on one side by a short loop element, termed ADP-ribosylating toxin turn turn (ARTT) motif [16]. The ARTT-motif harbors key catalytic residues, a C-terminally located glutamate, termed "catalytic glutamate" and a glutamine residue two positions upstream (QXE-motif), as well as a phenylalanine or tyrosine possibly involved in substrate recognition. The ARTT loop is found in many other ADP-ribosylating toxins, e.g. cholera toxin, pertussis toxin, actin-modifying *C. botulinum* C2-toxin and the *Pseudomonas aeruginosa* toxins ExoS and ExoT and is suggested to be involved in substrate recognition [16,22,23]. Here we report the crystal structure at 1.8 Å of the *C. limosum* C3 transferase and compare it to the structures of other family members.

2. Materials and methods

2.1. Protein production

C3lim (residues 1–205) without the N-terminal 45 amino acid signal sequence (residues −44 to 0) was expressed as a glutathione *S*-transferase (GST)-fusion protein. The gene encoding for residues 1–205 of *C. limosum* ADP-ribosyltransferase C3lim was cloned into vector pGEX-2TGL containing a glycine linker cloned with BglII/BamHI sticky ends into the BamHI site of pGEX-2T. The vector was cut with BamHI and

0014-5793/$34.00
doi:10.1016/j.febslet.2008.02.051

EcoRI and the C3 fragment introduced. The resulting construct contained an N-terminal GST tag, followed by a thrombin cleavage site and a 10 amino acid linker before the native C3lim sequence. Following thrombin cleavage (see below) the artificially tagged construct thus contained an N-terminal 12 amino acid extension (GSPGISGGGGGS).

For expression of recombinant C3lim the protein was overproduced at 37 °C for 10–12 h in the *Escherichia coli* strain BL21 (Stratagene, La Jolla, CA) after induction with 0.2 mM isopropyl-D-thiogalactoside. Cells were harvested by centrifugation, resuspended in lysis buffer (20 mM Tris/HCl (pH 7.5), 10 mM NaCl, 5 mM $MgCl_2$ and 1 mM PMSF) and broken with a French press (SLM Aminco, Spectronic Instruments). The lysate was centrifuged for 30 min at $15000 \times g$. The supernatant was incubated with glutathione-sepharose beads for 60 min at 4 °C to bind the GST-fusion protein. Beads were washed with buffer containing 50 mM Tris/HCl (pH 7.5) and 150 mM NaCl. The GST-fused C3lim protein was cleaved from the beads with thrombin (Sigma) in a buffer containing 50 mM TRIS/HCl (pH 7.5), 150 mM NaCl, 5 mM $CaCl_2$ and 5 mM TEA and further purified by size exclusion chromatography (Superdex 75, Amersham) in buffer-S (20 mM TRIS/HCl (pH 7.5), 150 mM NaCl, and 5 mM β-mercaptoethanol).

2.2. Crystallization, data collection and processing

Crystals of C3lim were grown at 20 °C by sitting drop vapour diffusion with drops mixed from 1 μL protein at 10 mg/mL in buffer-S and 1μL reservoir solution consisting of 0.2 M ammonium sulfate and 30% w/v polyethylene glycol 8000. In the cryo-protectant 20% glycerol was added. Crystals were flash frozen in a 100 K nitrogen stream, after soaking ~5 s in the cryo-protectant. A high resolution data set was collected at 100 K on the PX-1 beamline at the SLS (Villigen, CH). The diffraction data were processed with XDS [24]. Statistics of the data processing are shown in Table 1.

2.3. Structure determination and refinement

The structure of C3lim was solved with the molecular replacement method. As search models we used the coordinates of unliganded C3bot1 (PDB ID 1G24). Calculations were performed with program Molrep from the CCP4 suite [25] and resulted in unambiguous signals for two monomers. The model of C3lim was semiautomatically built with arp–warp [26]. Subsequently missing residues were built using the program Xfit [27] and improved by iterative rounds of manual rebuilding and refinement with Refmac [28] and Buster (Global Phasing Ltd.). The final model has been completed to residues 1–205 of C3lim, one sulphate ion and 219 water molecules. As defined by PROCHECK there are 92.9 % of residues in the most favored regions of the Ramachandran plot and 7.1 % in additionally allowed regions. The final statistics for the model are listed in Table 1. The program PyMOL (DeLano Scientific LLC) was used for figure preparation and structural analysis (RMSD calculations and distance measurements). Coordinates and structure factors have been deposited in the Protein Data Bank (PDB ID 3BW8).

Table 1
Data collection and refinement statistics

Data set[a]	C3lim
Space group	$P2_1$
Cell dimensions *a*, *b*, *c* (Å)	40.0, 91.5, 70.9
β (°)	106.5
Resolution (Å)	30–1.80 (1.90–1.80)
Observed reflections	77583
Unique reflections	40980
Completeness (%)	90.4 (72.2)
R_{sym}[b] (%)	8.2 (36.0)
$\langle I/\sigma(I)\rangle$	6.11 (2.3)
(R_{work}/R_{free})[c] (%)	19.5/23.4
Number of refined atoms	3439
Average *B*-factor (Å)[b]	28.4
Rms deviation	
Bond length (Å)	0.010
Bond angles (Å)	1.196

[a]Values in parentheses are for the highest resolution shell.
[b]$R_{sym} = \Sigma_{hkl}\Sigma_i|I_i - \langle I\rangle|/\Sigma_{hkl}\Sigma_i I_i$.
[c]$R_{work} = \Sigma_{hkl}\|F_{obs}| - k|F_{calc}\|/\Sigma_{hkl}|F_{obs}|$, R_{free} was calculated using 5% of data excluded from refinement.

3. Results and discussion

3.1. Structure determination

Crystals of C3lim grew under several non-redundant conditions (data not shown) with the best crystals obtained in space group $P2_1$ and two molecules in the asymmetric unit (designated as monomers A and B, respectively). A model of C3bot1 (with non-conserved residues truncated to alanine) was used to identify a molecular replacement solution. Electron density maps, calculated using phases from the molecular replacement solution showed clear difference electron density for side chains of residues that were not included in the search model. The model of C3lim was refined to a resolution of 1.8 Å with an R_{free} value of 23.4% and consists of residues 1–205 of C3lim (Table 1). A representative portion of the final electron density is shown in Fig. 1A. The catalytically important ARTT loop (see below) has clearly defined electron density in monomer A, whereas residues 169–172 could not be resolved in monomer B.

3.2. Structure description

The current model covers the entire polypeptide chain of C3lim, which folds into a mixed α/β-structure (Fig. 1B) similar as observed in previously solved structures of ADP-ribosylating toxins (Fig. 1C and Supplementary Fig. S1). Five α-helices surround a β-sandwich core, comprising a five-stranded mixed β-sheet (β1, β4, β8, β7, β2) and a three-stranded antiparallel β-sheet (β3, β6, β5). The sheets are aligned in a perpendicular orientation, causing a cleft in the overall structure, which is

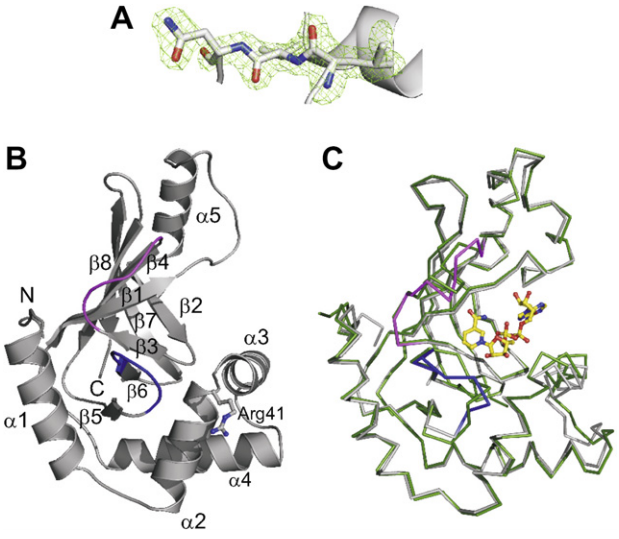

Fig. 1. Structure of C3lim and comparison with other C3 exoenzymes. (A) $|F_o| - |F_c|$ omit map for residues Leu137 to Asn139 of the PN loop. The electron density is contoured at 3.0 σ (green). (B) Ribbon diagram of C3lim. The catalytic ARTT and PN loops are colored blue and magenta. Arg41 is shown as a ball-and-stick representation. Secondary structure elements and N- and C-termini are indicated. (C) Superimposition of C3lim (backbone trace, color coded as in B) and C3bot1-NAD (PDB ID 1GZF, chain A, green). NAD is shown as a ball-and-stick representation (yellow).

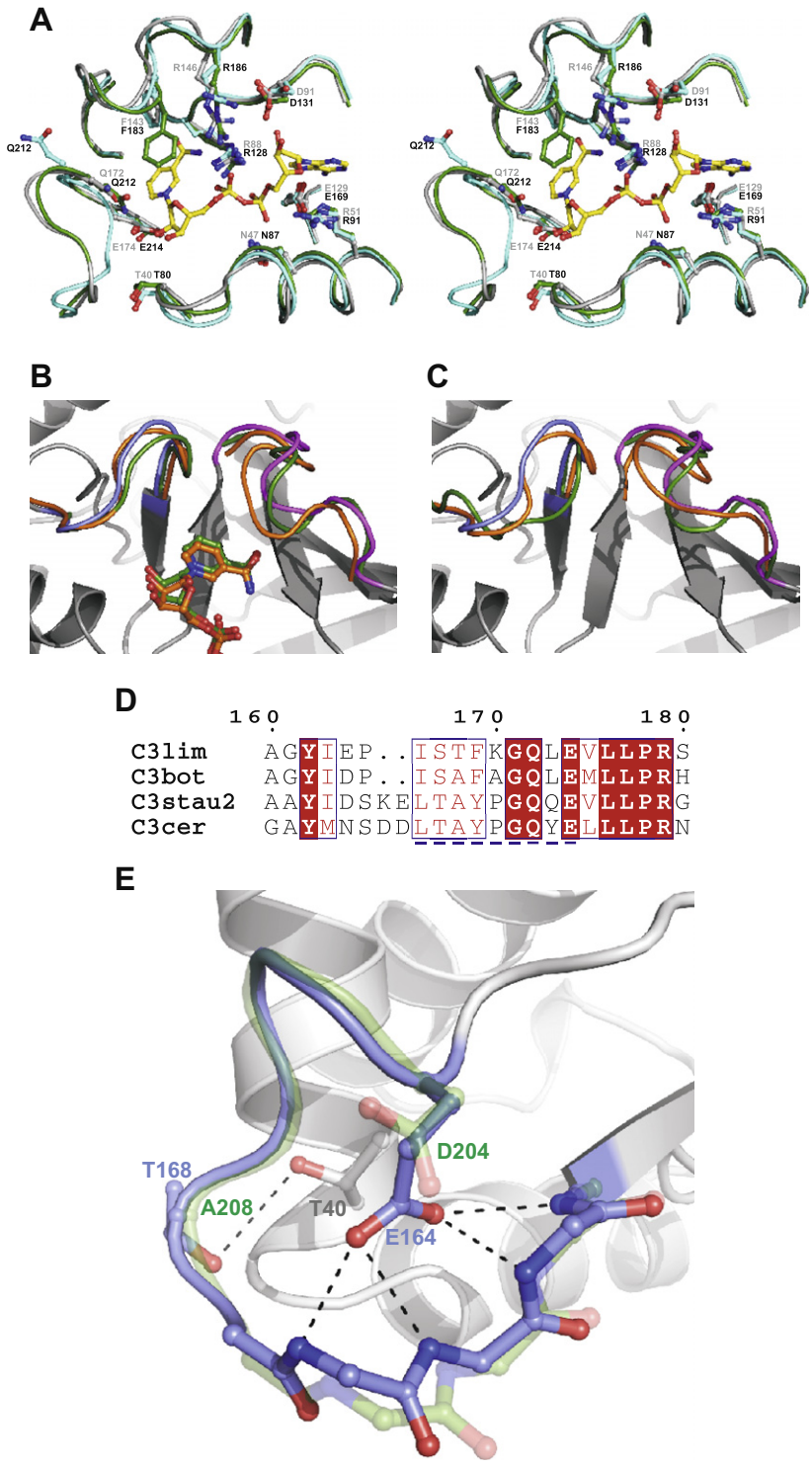

Fig. 2. Comparison with other C3 exoenzymes. (A) Stereo view of a structural overlay of the NAD binding pockets of C3lim (grey), C3bot1 (PDB ID 1G24, chain D, cyan) and C3bot1-NAD (PDB ID 1GZF, chain A, green). Backbone traces are presented as worms. Residues of C3bot1 which participate in NAD (yellow) interaction are presented as ball and stick model and are labeled in black. Corresponding amino acids of C3lim are indicated and labeled in grey. (B and C) Comparison of PN- and ARTT loops of C3 toxins. The ARTT loop (blue) and PN loop (magenta) of C3lim (grey) are superimposed with PN- and ARTT loops of C3bot1 (green) and C3stau2 (orange) in the NAD bound (B) and NAD free (C) conformations. The analysis is based on the following PDB entries: C3bot1, 1G24, chain D; C3bot1-NAD, 1GZF, chain A; C3stau2, 1OJQ; C3stau2-NAD, 1OJZ. (D) Sequence alignment of the catalytic ARTT loops (underlined in blue). The numbering refers to C3lim. (E) Stabilization of the C3lim ARTT loop. The ARTT loop of C3lim (blue) in its NAD free conformational state is stabilized by the side chain of Glu164 which forms polar interactions (cut-off level 3.5 Å, black dotted lines) with main chain amides of residues 171–174. Also indicated is an additional polar contact between Thr168 and Thr40 of α1. The ARTT loop of C3bot1 in its NAD bound state is superimposed (translucent green). The side chains $Asp204_{C3bot1}$, and $Ala208_{C3bot1}$ (green labels) which are in corresponding positions to $Glu164_{C3lim}$, and $Thr168_{C3lim}$ (blue labels) are indicated.

partially shielded by the helical segments α2–α4. This spatial arrangement provides the structural basis of the NAD binding pocket as shown by the crystal structures of the NAD bound form of related toxins like C3bot1 and C3stau2, which show only minor structural differences to C3lim. Superimposition of C3lim with the NAD free conformations of C3bot1 (PDB ID 1G24, chain D) and C3stau2 (PDB ID 1OJQ) reveals low root mean square deviations (r.m.s.d) of 0.54 and 1.25 Å, respectively (Supplementary Fig. S1). Therefore, we assume an identical NAD binding mode for C3lim. In fact, a structural overlay of the catalytic core region of C3bot1 bound to NAD (PDB ID 1GZF, chain A) with the NAD free form of C3lim reveals that amino acids of C3lim, which correspond to residues participating in NAD–C3bot1 interaction are almost identically positioned with an r.m.s.d. of 0.535 Å (Fig. 2A and B). The structural similarity corresponds well to the primary sequence identities of 61% for C3bot1 and 34% for C3stau2, respectively. Within the NAD binding region, differences occur within the PN loop (residues 137–146) and ARTT loop (residues 166–174), which show slightly different conformations. Interestingly, the catalytic ARTT loop of C3lim (monomer A) adopts a conformation, which resembles the NAD bound ARTT loop of C3bot1 much more (Fig. 2B) than its NAD free counterpart (Fig. 2C). A similar observation has been described for C3stau2 [18] whose ARTT loop conformation is not dependent on NAD interaction (Fig. 2B and C). In the latter case a two amino acid insertion flanking the N-terminal ARTT loop region seems to be responsible for the invariant conformation (Fig. 2D). There is no comparable insertion in C3lim, but a detailed inspection of the ARTT loop reveals a set of polar interactions which are unique compared to C3bot1 (Fig. 2E). The side chain of Glu164 is suitably arranged to interact with main chain amides of residues 171–174. The corresponding residue in C3bot1 is an aspartate, the side chain of which is too short to form such a polar network. An additional interaction is formed between Thr168 and Thr40 of helix α2, which might also contribute to stabilization of the ARTT loop. In contrast, in C3bot1 both residues are replaced by alanine.

In summary, the C3lim crystal structure further generalizes our understanding of C3 toxins and their structure-activity relationships. Whereas the overall structure is similar to the known C3 toxins, we observe the ARTT-motif in a unique, pre-stabilized conformation that resembles C3stau2 more than C3bot1.

3.3. Biochemical implications

The biochemical analysis of C3stau2 identified the atypical Rho proteins RhoE/Rnd3 as a unique substrate protein in addition to RhoA [11]. This modification was in part explained by the fixed conformation and a different length of the C3stau2 ARTT loop (Fig. 2D) [11,18]. Structural analysis of C3lim revealed an ARTT loop conformation that is already primed for NAD binding, similar to apo-C3stau2 but different from apo-C3bot1. Because C3lim does not modify RhoE, it is unlikely that the ARTT loop conformation found in C3stau2 and C3lim define the extended substrate modifications typical for C3stau2.

Glu174 of C3lim, which is located at the C-terminal end of the ARTT loop (Fig. 2A and D), is the so-called "catalytic glutamic acid" residue, which is conserved in all ADP-ribosyltransferases studied so far [2,29]. Two amino acid residues up-stream of the catalytic glutamate is a glutamine residue, which is conserved in all C3-like exoenzymes forming the EXQ-motif. This motif is changed to EXE in all known arginine-modifying ADP-ribosyltransferases including for example the G_S-protein-modifying cholera toxin and the actin-modifying binary ADP-ribosylating toxins like *C. botulinum* C2 toxin [29]. Recently it has been reported that change of the EXQ-motif of C3lim to EXE inhibits RhoA ADP-ribosylation at asparagine but favors modification of arginine residues in polyarginine [21]. Moreover, it was shown that EXE-C3lim ($Q172E_{C3lim}$) is modified by intra- and inter-molecular auto-ADP-ribosylation at arginine residues. The major modification occurs at $Arg41_{C3lim}$ in an intermolecular manner [21]. More importantly, ADP-ribosylation of C3lim at Arg41 largely reduced its activity to ADP-ribosylate RhoA [21]. The crystal structure of C3lim allows major insights into the role of Arg41. This residue, which is located in helix 2, is unique in the group of C3-like transferases. It is located in helix2 at the connection to helix 3 (Fig. 1B). The crystal structure reveals the surface orientation of $Arg41_{C3lim}$ in helix 2. Helix 3 has been suggested to be involved in substrate recognition. Deduced from the structure of the related *Clostridium perfringens* iota toxin, which modifies actin, it has been suggested that Ser40 and Asn44 in C3stau2 are involved in protein substrate recognition [18]. Ser40 is equivalent to Ala43 in C3lim and located in helix2, whereas Asn44 of C3stau2 is equivalent to Asn47 in C3lim located in helix3. Also studies on the substrate specificity of *Pseudomonas exoenzyme* S and T reveal that the region covering the C-terminal part of helix2 and the N-terminal part of helix3, which is directly located at the NAD binding cleft, form an "active site loop" (from Tyr272-Asn281) crucial for substrate recognition [30]. Deduced from the structure of C3lim shown here it is plausible that attachment of ADP-ribose to $Arg41_{C3lim}$ could interfere with toxin-substrate interactions and explain the observed drop in the enzymatic activity. In conclusion $Arg41_{C3lim}$ represents a potential modulation site for the enzymatic activity of the transferase and is a unique characteristic of C3lim.

Acknowledgements: Clemens Schulze-Briese and the beamline staff of SLS-PX1 are acknowledged for support during data collection.

Appendix A. Supplementary data

Supplementary data associated with this article can be found, in the online version, at doi:10.1016/j.febslet.2008.02.051.

References

[1] Krueger, K.M. and Barbieri, J.T. (1995) The family of bacterial ADP-ribosylating exotoxins. Clin. Microbiol. Rev. 8, 34–47.
[2] Glowacki, G., Braren, R., Firner, K., Nissen, M., Kuhl, M., Reche, P., Bazan, F., Cetkovic-Cvrlje, M., Leiter, E., Haag, F. and Koch-Nolte, F. (2002) The family of toxin-related ecto-ADP-ribosyltransferases in humans and the mouse. Protein Sci. 11, 1657–1670.
[3] Just, I., Hofmann, F., Genth, H. and Gerhard, R. (2001) Bacterial protein toxins inhibiting low-molecular-mass GTP-binding proteins. Int. J. Med. Microbiol. 291, 243–250.
[4] Aktories, K. and Barbieri, J.T. (2005) Bacterial cytotoxins: targeting eukaryotic switches. Nat. Rev. Microbiol. 3, 397–410.

[5] Aktories, K., Wilde, C. and Vogelsgesang, M. (2004) Rho-modifying C3-like ADP-ribosyltransferases. Rev. Physiol. Biochem. Pharmacol. 152, 1–22.
[6] Vogelsgesang, M., Pautsch, A. and Aktories, K. (2007) C3 exoenzymes, novel insights into structure and action of Rho-ADP-ribosylating toxins. Naunyn Schmiedebergs Arch. Pharmacol. 374, 347–360.
[7] Aktories, K., Weller, U. and Chhatwal, G.S. (1987) *Clostridium botulinum* type C produces a novel ADP-ribosyltransferase distinct from botulinum C2 toxin. FEBS Lett. 212, 109–113.
[8] Just, I., Mohr, C., Schallehn, G., Menard, L., Didsbury, J.R., Vandekerckhove, J., van Damme, J. and Aktories, K. (1992) Purification and characterization of an ADP-ribosyltransferase produced by *Clostridium limosum*. J. Biol. Chem. 267, 10274–10280.
[9] Just, I., Selzer, J., Jung, M., van Damme, J., Vandekerckhove, J. and Aktories, K. (1995) Rho-ADP-ribosylating exoenzyme from *Bacillus cereus* – purification, characterization and identification of the NAD-binding site. Biochemistry 34, 334–340.
[10] Sugai, M., Enomoto, T., Hashimoto, K., Matsumoto, K., Matsuo, Y., Ohgai, H., Hong, Y.-M., Inoue, S., Yoshikawa, K. and Suginaka, H. (1990) A novel epidermal cell differentiation inhibitor (EDIN): purification and characterization from *Staphylococcus aureus*. Biochem. Biophys. Res. Commun. 173, 92–98.
[11] Wilde, C., Chhatwal, G.S., Schmalzing, G., Aktories, K. and Just, I. (2001) A novel C3-like ADP-ribosyltransferase from *Staphylococcus aureus* modifying RhoE and Rnd3. J. Biol. Chem. 276, 9537–9542.
[12] Sekine, A., Fujiwara, M. and Narumiya, S. (1989) Asparagine residue in the rho gene product is the modification site for botulinum ADP-ribosyltransferase. J. Biol. Chem. 264, 8602–8605.
[13] Aktories, K., Braun, U., Rösener, S., Just, I. and Hall, A. (1989) The rho gene product expressed in *E. coli* is a substrate of botulinum ADP-ribosyltransferase C3. Biochem. Biophys. Res. Commun. 158, 209–213.
[14] Chardin, P., Boquet, P., Madaule, P., Popoff, M.R., Rubin, E.J. and Gill, D.M. (1989) The mammalian G protein rho C is ADP-ribosylated by *Clostridium botulinum* exoenzyme C3 and affects actin microfilament in Vero cells. EMBO J. 8, 1087–1092.
[15] Paterson, H.F., Self, A.J., Garrett, M.D., Just, I., Aktories, K. and Hall, A. (1990) Microinjection of recombinant $p21^{rho}$ induces rapid changes in cell morphology. J. Cell Biol. 111, 1001–1007.
[16] Han, S., Arvai, A.S., Clancy, S.B. and Tainer, J.A. (2001) Crystal structure and novel recognition motif of Rho ADP-ribosylating C3 exoenzyme from *Clostridium botulinum*: structural insights for recognition specificity and catalysis. J. Mol. Biol. 305, 95–107.
[17] Ménétrey, J., Flatau, G., Stura, E.A., Charbonnier, J.-B., Gas, F., Teulon, J.-M., Le Du, M.-H., Boquet, P. and Ménez, A. (2002) NAD binding induces conformational changes in Rho ADP-ribosylating *Clostridium botulinum* C3 exoenzyme. J. Biol. Chem. 277, 30950–30957.
[18] Evans, H.R., Sutton, J.M., Holloway, D.E., Ayriss, J., Shone, C.C. and Acharya, K.R. (2003) The crystal structure of C3stau2 from *Staphylococcus aureus* and its complex with NAD. J. Biol. Chem. 278, 45924–45930.
[19] Böhmer, J., Jung, M., Sehr, P., Fritz, G., Popoff, M., Just, I. and Aktories, K. (1996) Active site mutation of the C3-like ADP-ribosyltransferase from *Clostridium limosum* – analysis of glutamic acid 174. Biochemistry 35, 282–289.
[20] Wilde, C., Genth, H., Aktories, K. and Just, I. (2000) Recognition of RhoA by *Clostridium botulinum* C3 exoenzyme. J. Biol. Chem. 275, 16478–16483.
[21] Vogelsgesang, M. and Aktories, K. (2006) Exchange of glutamine-217 to glutamate of *Clostridium limosum* exoenzyme C3 turns the asparagine-specific ADP-ribosyltransferase into an arginine-modifying enzyme. Biochemistry 45, 1017–1025.
[22] Han, S. and Tainer, J.A. (2002) The ARTT motif and a unified structural understanding of substrate recognition in ADP-ribosylating bacterial toxins and eukaryotic ADP-ribosyltransferases. Int. J. Med. Microbiol. 291, 523–529.
[23] Barbieri, J.T. and Sun, J. (2004) Pseudomonas aeruginosa ExoS and ExoT. Rev. Physiol. Biochem. Pharmacol. 152, 79–92.
[24] Kabsch, W. (1993) Automatic processing of rotation diffraction data from crystals of initially unknown symmetry and cell contents. J. Appl. Cryst. 26, 795–800.
[25] Collaborative Computational Project No. 4 (1994) The CCP4 suite: programs for protein crystallography. Acta Crystallogr. D. 50, 760–763.
[26] Morris, R.J., Perrakis, A. and Lamzin, V.S. (2003) ARP/wARP and automatic interpretation of protein electron density maps. Methods Enzymol. 374, 229–244.
[27] McRee, D.E. (1999) XtalView/Xfit–A versatile program for manipulating atomic coordinates and electron density. J. Struct. Biol. 125, 156–165.
[28] Murshudov, G.N., Vagin, A.A. and Dodson, E.J. (1997) Refinement of macromolecular structures by the maximum-likelihood method. Acta Crystallogr. D. 53, 240–255.
[29] Holbourn, K.P., Shone, C.C. and Acharya, K.R. (2006) A family of killer toxins. Exploring the mechanism of ADP-ribosylating toxins. FEBS J. 273, 4579–4593.
[30] Sun, J., Maresso, A.W., Kim, J.J. and Barbieri, J.T. (2004) How bacterial ADP-ribosylating toxins recognize substrates. Nat. Struct. Mol. Biol. 11, 868–876.